Molecular Transport

DOI: 10.1002/ange.200504579

Surfactant-Modulated Switching of Molecular Transport in Nanometer-Sized Pores of Membrane Gates

*Riaan Schmuhl, Albert van den Berg, Dave H. A. Blank, and Johan E. ten Elshof**

Molecular and ionic gates through which species can be transported at will under the influence of externally tunable parameters have received considerable attention recently.[1–7] In view of their relevance for application in microfluidic devices, these components are becoming an established

[*] Dr. R. Schmuhl, Prof. D. H. A. Blank, Dr. J. E. ten Elshof
Inorganic Materials Science
MESA+ Institute for Nanotechnology
University of Twente
7500 AE, Enschede (The Netherlands)
Fax: (+31) 53-489-4683
E-mail: j.e.tenelshof@utwente.nl
Prof. A. van den Berg
Laboratory of Biosensors
MESA+ Institute for Nanotechnology
University of Twente
7500 AE, Enschede (The Netherlands)

Supporting information for this article is available on the WWW under http://www.angewandte.org or from the author.

technology in analytical chemistry and biotechnology.[8,9] They may enable new ways of molecular separation, dosing, and analysis.[1–7] The channels or pores of the gate typically have diameters of ≈20 nm or less in order to function properly. The operating principle is based on the presence of 1) a driving force for species transport, usually a concentration or electrical potential gradient over the gate, and 2) an externally controllable switch with which the gate can be opened or closed, or the selectivity of the gate modified.

Martin and co-workers were the first to show the concept of influencing the ion permselectivity of nanoporous nuclear-track-etched polymeric membranes by imposing an electrical bias potential (relative to the feed solution) on the gold-coated inner pore surface of the membrane.[2] We and others demonstrated that the selectivity of a membrane toward anions or cations can also be controlled by adjusting the ionic strength and pH of the system, which results in the electrostatic opening and closing of membrane pores.[1–9] Alternatively, Sweedler, Bohn, and co-workers developed a gateable interconnect for analyte injection in microfluidic devices,[1,4] where transport is driven by electroosmotic flow and the selectivity is determined by the double-layer properties inside the pore. It has also been shown that modification of the membrane surface properties by self-assembled monolayers of amino- or carboxy-functional molecules imparts to the membrane a high dependency of the ionic permeability on the pH value.[10–12]

In a number of recent studies, the transport behavior of ionic species in nanometer-sized pores has been modeled to gain a better understanding of the influence of the double layer and surface charge density on the ion-transport properties.[13–15] However, the control of ionic strength and surface charge to manipulate the permeability of a membrane is limited to dilute conditions under which double-layer overlap inside the channel/pore occurs, that is, at relatively low ionic strengths, when charge exclusion is sufficient to reject ions.[5–7] A much more universal method of tuning the permeability of molecular gates would be the controlled steric blocking of permeating species. By physically blocking or unblocking the channels of a gate, an open/closed system can be created. This concept could also be useful, for instance, when species are present whose structure and function depend on ionic strength and pH, such as enzymes.

We illustrate the concept with a tunable membrane gate, the working principle of which is essentially based on the co-addition of surfactant molecules to a system of ionic probes that are transported through a membrane under the influence of an electrical potential gradient. As a result of their size and ability to adsorb reversibly inside channels and pores, these surfactants can be used to physically open or close nanometer-sized channels and pores of molecular gates by varying their concentration. Thus, the flux of ionic or molecular species can be controlled by an independent, externally tunable variable, without having to manipulate the probe concentration in the feed or the driving force for transport.

A four-region adsorption model has been proposed to explain the adsorption of surfactants at charged interfaces depending on concentration.[16] Adsorption can occur either directly on an oppositely charged interface or through oppositely charged counterions.[17] At an increasing concentration, the adsorption characteristics range from isolated monomers through local aggregates to complete monolayers, bilayers, and ultimately to hemicelles (see Figure 1 a). The application of surfactants thus offers the possibility of chemically modifying the internal channel surface,[18] and of influencing the net electrostatic charge present on the pore walls. The exact structure of the adsorbed surfactant layer determines how pore size, pore chemistry, and surface charge density are affected by adsorption. Three surfactants were used in the present study (Figure 1 b): cetyltrimethylammonium bromide (CTAB), sodium dodecyl sulfate (SDS), and triethylhexylammonium bromide (C6TEA). These compounds have carbon tail lengths of 16, 12, and 6, respectively. An α-alumina-supported γ-alumina membrane gate was placed in a U-shaped tube, and external Pt electrodes were fixed on both sides of the membrane over which the driving force was applied.[6] Ionic probes were introduced on one side (feed) of the gate, and surfactants were added on both the feed and receive sides at the same concentration.

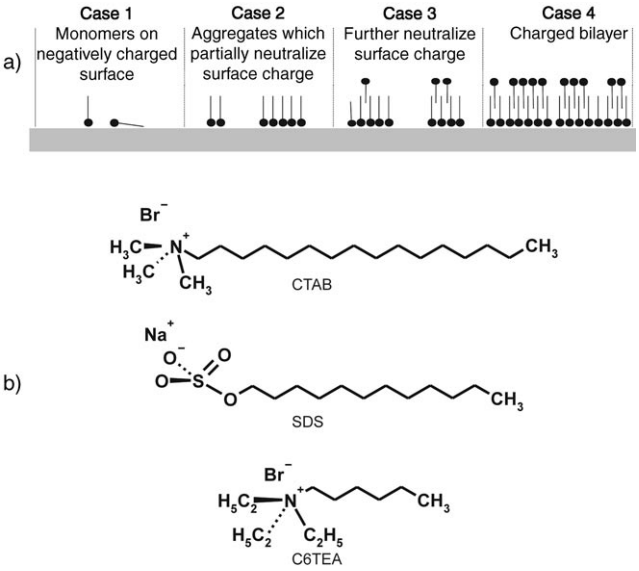

Figure 1. a) Schematic representation of the adsorption behavior of surfactants at varying concentrations according to the four-region adsorption model. b) Structures of the surfactants used: cetyltrimethylammonium bromide (CTAB), sodium dodecyl sulfate (SDS), and triethylhexylammonium bromide (C6TEA).

Figure 2 shows the influence of surfactant concentration on the flux of doubly charged methyl viologen cations (MV^{2+}) and fluorescein anions (Fl^{2-}). The surfactant concentrations were increased at 24-hour intervals after steady-state conditions had been reached. The gray bands in the figure indicate the average steady-state fluxes of probe ions through the gate when no surfactant was present. When long-chain CTAB or SDS were used, the MV^{2+} flux could be suppressed with surfactant concentrations larger than $\approx 10^{-4}$ M. A qualitatively similar, though less pronounced trend was observed in the presence of short-chain C6TEA. When the same surfactants were used together with Fl^{2-} ions, the flux of the

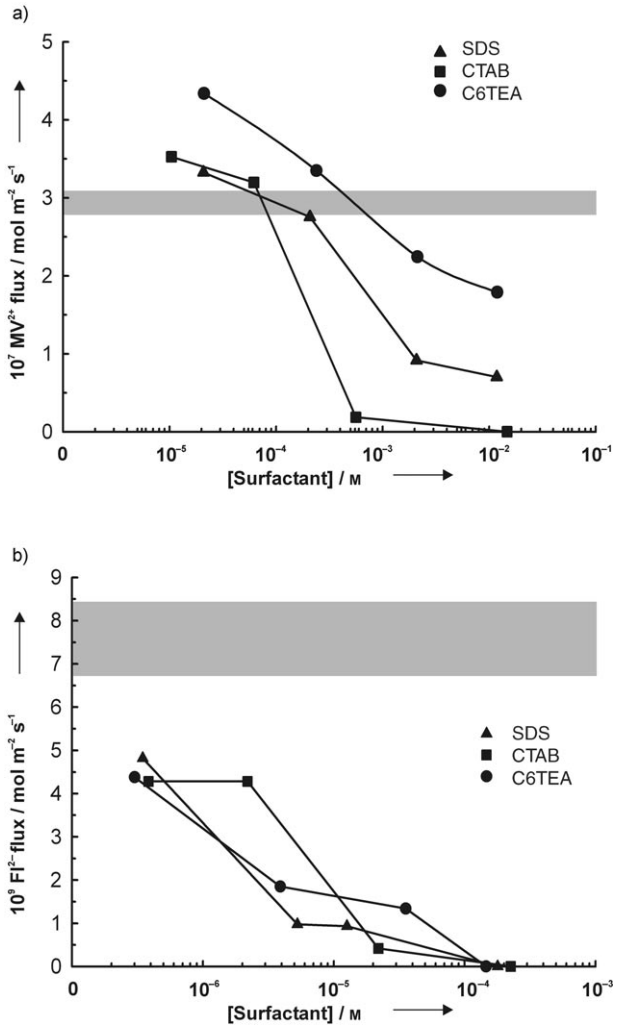

Figure 2. Influence of surfactant concentration on transport rate of a) methyl viologen cations (MV^{2+}) and b) fluorescein anions (Fl^{2-}) through an α/γ-alumina membrane gate. [MV^{2+}] and [Fl^{2-}] at feed side is 8×10^{-4} M. The potential difference ΔV over the membrane is -2 and $+2$ V, respectively. The gray area represents the average flux of the ionic probes when no surfactant was present in the system.

ionic probes decreased in all cases and became virtually zero above 10^{-4} M, irrespective of the type of surfactant used.

The open/close switching ability of the membrane by co-addition of surfactant molecules at the feed side and its effect on the flux of MV^{2+} and Fl^{2-} is illustrated by the enhancement factor R, which is defined as the ratio of the ionic flux in the presence and absence of surfactant. Selected values of R at high and low concentrations are listed in Table 1. Partial or complete pore blocking ($R<1$) was observed for both probe molecules when the surfactant concentration was sufficiently high. The degree to which the flux can be controlled depends on the nature and concentration of the surfactant; however, for both probe molecules the degree of blocking at high concentration increased in the sequence C6TEA < SDS < CTAB. After surfactant removal the transport rates were restored to their original values. Hence, the pores can be reversibly opened and closed for ion transport. The magnitude of the ionic fluxes can be controlled completely by addition of surfactant. The desorption process was somewhat slow and seems to be controlled by a limited mass-transfer rate.

The influence of surfactant on the ionic probes can be exerted through the electrostatic charge of the polar head groups and/or by the length of the hydrophobic tail. When considering the differences between the cationic surfactants CTAB and C6TEA, which have the same head groups, the tail length clearly has an influence: CTAB is more effective than C6TEA in suppressing the MV^{2+} flux at a high surfactant concentration, and is roughly as effective as SDS. This finding suggests that the adsorption of long-chain surfactants causes steric effects to play a substantial role in the blocking process.

However, an alternative explanation could be that the small fluxes at high surfactant concentrations are a result of the formation of molecule–surfactant complexes. To rule out this possibility, MV^{2+} solutions were investigated by UV/Vis spectroscopy in the presence of different concentrations of surfactants. No significant changes were observed in the spectra, except at very high concentrations of SDS ($\approx10^{-2}$ M), in which a shift in the absorption maximum was observed, which indicates that there was some interaction between MV^{2+} ions and SDS. As regards Fl^{2-} ions, fluorescence spectroscopy showed no evidence of a surfactant–Fl^{2-} interaction. Hence, steric hindrance of ion transport by surfactants appears to be the dominant mechanism of permeability control at high concentration.

Surprisingly, an enhancement of the MV^{2+} flux ($R>1$) was observed in the presence of low surfactant concentrations (10^{-6}–10^{-4} M; see Figure 1b and Table 1). Apparently, the mobility and/or local concentration of MV^{2+} ions are affected by a low concentration of adsorbed surfactants. Several factors might play a role, although it seems likely that the rate enhancement is somehow related to a (partial) screening of the native charges present on the alumina surface, and the more aliphatic nature of the pore walls after surfactant adsorption. At the low concentrations of 10^{-4} M or less, at which $R>1$ occurred, a monolayer of surfactant is present on the membrane surface. The formation of surfactant aggregates at $\approx10^{-5}$ M (case 2 in Figure 1a) neutralizes the surface charge and increases the hydrophobicity of the alumina surface.[16,19] As the long-range coulombic interactions between charged surface sites and MV^{2+} lower the mobility of MV^{2+} ions inside the pore, the partial screening of surface charges by adsorbed surfactants will increase the MV^{2+} ionic mobility. In addition, the more aliphatic nature of the pore probably provides more favorable surroundings for MV^{2+} ions than the bulk water phase, so that MV^{2+} partitions preferentially into the membrane, thus leading to a higher concentration inside the pore. Both effects will enhance the ion transport rate. C6TEA was more effective in enhancing the flux of MV^{2+} than CTAB or SDS. This finding is probably explained by the smaller size of C6TEA, as it may be able to adsorb in and around charged surface sites where the larger CTAB and SDS could be sterically hindered. No enhancement factors $R>1$ were observed for Fl^{2-}, which may be related to the fact that it is a less hydrophobic ion than MV^{2+}.

Figure 3 shows the zeta potential of γ-alumina as a function of surfactant concentration.[20] This experiment

Table 1: Ionic fluxes and enhancement factors (R) of MV^{2+} and Fl^{2-} through a γ-alumina membrane gate upon co-addition of surfactant.[a]

Surfactant	Concentration [M]	MV^{2+}		Fl^{2-}	
		Flux [$mol\,m^{-2}\,s^{-1}$]	R	Flux [$mol\,m^{-2}\,s^{-1}$]	R
None	0	$(2.8–3.2)\times10^{-7}$	1	$(6.9–8.4)\times10^{-9}$	1
SDS	10^{-5}	3.3×10^{-7}	1.11	4.5×10^{-9}	0.59
	10^{-3}			$<7.2\times10^{-15}$	$<10^{-6}$
	10^{-2}	7.8×10^{-9}	0.026		
CTAB	10^{-6}			5.8×10^{-9}	0.76
	10^{-5}	3.5×10^{-7}	1.18		
	10^{-3}			$<7.2\times10^{-15}$	$<10^{-6}$
	10^{-2}	1.8×10^{-9}	0.006		
C6TEA	10^{-5}	4.3×10^{-7}	1.44		
	10^{-4}			5.9×10^{-9}	0.77
	10^{-3}			$<7.2\times10^{-15}$	$<10^{-6}$
	10^{-2}	2.0×10^{-7}	0.68		

[a] The potential difference ΔV over the membrane is -2 and $+2$ V for MV^{2+} and Fl^{2-} ions, respectively. ΔV is defined as $\Delta V = V_{receive} - V_{feed}$, where V_{feed} and $V_{receive}$ are the electrode potentials at the feed and receive sides, respectively. The membrane was placed between the two halves of a U-shaped tube with the oxide layer exposed to the so-called feed side. $[MV^{2+}]$ and $[Fl^{2-}]$ at feed side is 8×10^{-4} M.

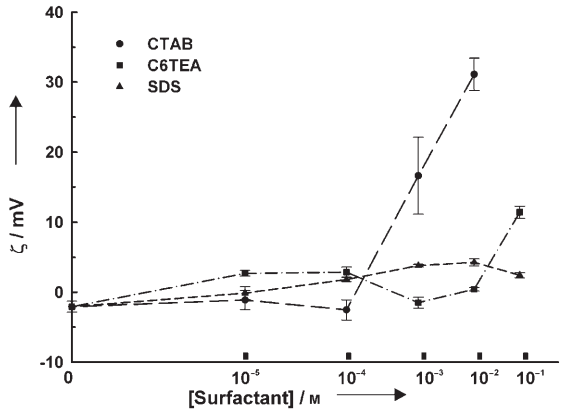

Figure 3. Zeta potential of γ-alumina powder as a function of surfactant concentration in the presence of phosphate buffer (pH 6). Conditions are similar to those for the permeability measurements. Lines serve as a guide to the eye.

provides insight into the effect of surfactant adsorption on alumina surface charge, and may thus help to distinguish steric and charge-blocking effects more clearly. In the absence of surfactant the zeta potential was slightly negative. At low concentrations the potentials varied slightly depending on the concentration and nature of the surfactant. The sudden strong increase of the zeta potential of solutions containing CTAB and C6TEA at concentrations of $\approx10^{-3}$ and 10^{-1} M, respectively, indicates the formation of charged bilayers. The formation of a bilayer in the pores at high concentration (case 4 in Figure 1a) is likely to lead to both an increase of flux-retarding coulombic interactions between the charged surface and probe ion, and an increased steric hindrance of the probe ions inside the nanometer-sized pores because of the presence of a bilayer. In contrast, the zeta potential of SDS shows no indication of a charged bilayer up to at least 10^{-1} M. Yet, the MV^{2+} and Fl^{2-} fluxes at high concentration decrease in the order C6TEA > SDS > CTAB, and so SDS is a more effective transport-blocking surfactant than C6TEA. Apparently, the blocking of the ionic probe by SDS does not occur by an increase of coulombic interactions, but rather by steric hindrance. The data support the findings that SDS and CTAB block ion transport sterically because of their long hydrocarbon tails, and that CTAB and C6TEA block transport by coulombic interactions through a charged bilayer. CTAB is both a steric and coulombic pore blocker, and is thus the most effective surfactant at high concentrations, followed by SDS (mainly steric blocking) and C6TEA (mainly charge blocking).

In summary, a switchable membrane gate for ionic species that operates by co-addition and removal of surfactants was demonstrated. The permeability of the gate for ionic probe molecules could be manipulated by steric and/or coulombic blocking depending on the nature of the surfactant. The blocking and unblocking of pores was reversible, thus demonstrating a membrane gate with in situ tunable permeability. Under specific conditions, cation fluxes higher than in the absence of surfactant were observed. The kinetics of surfactant sorption seem to be controlled by mass transfer. Surface-active species may also complicate transport behavior in some cases. The ability to physically control the transport rate through the membrane gate by an externally tunable variable, which is independent of the probe ion concentration and driving force, provides an interesting approach that could find use in devices such as selective gates for DNA and protein sampling routines, injectors for electrophoretic separations, or on-demand therapeutic agents in microfluidic devices.

Received: December 23, 2005
Published online: April 10, 2006

Keywords: adsorption · membranes · molecular transport · nanopores · surfactants

[1] T.-C. Kuo, L. A. Sloan, J. V. Sweedler, P. W. Bohn, *Langmuir* **2001**, *17*, 6298–6303.
[2] M. Nishizawa, V. P. Menon, C. R. Martin, *Science* **1995**, *268*, 700–702.
[3] C. R. Martin, M. Nishizawa, K. Jirage, M. Kang, S. B. Lee, *Adv. Mater.* **2001**, *13*, 1351–1362.
[4] P. J. Kemery, J. K. Steehler, P. W. Bohn, *Langmuir* **1998**, *14*, 2884–2889.
[5] R. Schmuhl, J. Sekulić, S. Roy Chowdhury, C. J. M. van Rijn, K. Keizer, A. van den Berg, J. E. ten Elshof, D. H. A. Blank, *Adv. Mater.* **2004**, *16*, 900–904.
[6] R. Schmuhl, W. Nijdam, J. Sekulić, S. Roy Chowdhury, C. J. M. van Rijn, A. van den Berg, J. E. ten Elshof, D. H. A. Blank, *Anal. Chem.* **2005**, *77*, 178–184.
[7] R. Schmuhl, K. Keizer, A. van den Berg, J. E. ten Elshof, D. H. A. Blank, *J. Colloid Interface Sci.* **2004**, *273*, 331–338.

[8] T.-C. Kuo, H.-K. Kim, D. M. Cannon, Jr., M. A. Shannon, J. V. Sweedler, P. W. Bohn, *Angew. Chem.* **2004**, *116*, 1898 – 1901; *Angew. Chem. Int. Ed.* **2004**, *43*, 1862 – 1865.
[9] A. Plecis, R. B. Schoch, P. Renaud, *Nano Lett.* **2005**, *5*, 1147 – 1155.
[10] Z. Hou, N. L. Abbott, P. Stroeve, *Langmuir* **2000**, *16*, 2401 – 2404.
[11] K-Y. Chun, P. Stroeve, *Langmuir* **2002**, *18*, 4653 – 4658.
[12] S. B. Lee, C. R. Martin, *Anal. Chem.* **2001**, *73*, 768 – 775.
[13] A. N. Chatterjee, D. M. Cannon, E. N. Gatimu, J. V. Sweedler, N. R. Aluru, P. W. Bohn, *J. Nanopart. Res.* **2005**, *7*, 507 – 516.
[14] D. N. Petsev, *J. Chem. Phys.* **2005**, *123*, 244907.
[15] S. Pennathur, J. G. Santiago, *Anal. Chem.* **2005**, *77*, 6772 – 6781.
[16] A. Fan, P. Somasundaran, N. J. Turro, *Langmuir* **1997**, *13*, 506 – 510.
[17] L. J. Crisenti, D. A. Sverjensky, *Am. J. Sci.* **1999**, *299*, 828 – 899.
[18] A. A. Kavitskaya, N. A. Klimenko, A. V. Bildyukevich, A. A. Petrachkov, *Desalination* **2003**, *158*, 225 – 230.
[19] P. Chandar, P. Somasundaran, N. J. Turro, *J. Colloid Interface Sci.* **1987**, *117*, 31 – 46.
[20] W. B. S. de Lint, N. E. Benes, J. Lyklema, H. J. M. Bouwmeester, A. J. van der Linde, M. Wessling, *Langmuir* **2003**, *19*, 5861 – 5868.

